Toward a unified hydrous olivine electrical conductivity law

Emmanuel Gardès, Fabrice Gaillard, Pascal Tarits

AGU PUBLICATIONS

Geochemistry, Geophysics, Geosystems

RESEARCH ARTICLE

10.1002/2014GC005496

Key Points:
- Hydrous olivine electrical conductivity measurements are mostly consistent
- Our new hydrous olivine conductivity law best reproduces the database
- Upper mantle highest conductivities are unlikely due to olivine hydration

Correspondence to:
E. Gardés,
gardes@ganil.fr

Citation:
Gardés, E., F. Gaillard, and P. Tarits (2014), Toward a unified hydrous olivine electrical conductivity law, *Geochem. Geophys. Geosyst.*, *15*, doi:10.1002/2014GC005496.

Received 11 JUL 2014
Accepted 3 DEC 2014
Accepted article online 9 DEC 2014

Toward a unified hydrous olivine electrical conductivity law

Emmanuel Gardés[1,2,3,4], Fabrice Gaillard[2,3,4], and Pascal Tarits[5]

[1]CEA-CNRS-ENSICAEN-Université de Caen Basse Normandie, CIMAP, UMR 6252, Caen, France, [2]Université d'Orléans, ISTO, UMR 7327, Orléans, France, [3]CNRS/INSU, ISTO, UMR 7327, Orléans, France, [4]BRGM, ISTO, UMR 7327, Orléans, France, [5]Université de Bretagne Occidentale-CNRS, IUEM, UMR 6538, Plouzané, France

Abstract It has long been proposed that water incorporation in olivine has dramatic effects on the upper mantle properties, affecting large-scale geodynamics, and triggering high electrical conductivity. But the laboratory-based laws of olivine electrical conductivity predict contrasting effects of water, precluding the interpretation of geophysical data in term of mantle hydration. We review the experimental measurements of hydrous olivine conductivity and conclude that most of data are consistent when errors in samples water contents are considered. We report a new law calibrated on the largest database of measurements on hydrous olivine oriented single crystals and polycrystals. It fits most of measurements within uncertainties, and is compatible with most of geophysical data within petrological constraints on mantle olivine hydration. The conductivity anisotropy of hydrous olivine might be higher than dry olivine, but preferential orientation should produce moderate anisotropy (~0–0.8 log unit). In the oceanic mantle, the enhancement of olivine conductivity is limited to ~1 log unit in the maximum range of mantle olivine water concentrations (0–500 wt ppm). Strongest enhancements are expected in colder regions, like cratonic lithospheres and subduction settings. High conductivities in melt-free mantle require great depths and high water concentrations in olivine (>0.1 S/m at >250 km and >200 wt ppm). Thus, the hydration of olivine appears unlikely to produce the highest conductivities of the upper mantle.

1. Introduction

The interpretation of high electrical conductivities is a key step in the understanding of the global geodynamics in the upper mantle. The enhancement of upper mantle conductivities due to the incorporation of trace amounts of hydrogen in olivine, the dominant upper mantle phase, has been the most influencing hypothesis [*Karato*, 1990] with important geodynamics implications [*Hirth and Kohlstedt*, 1996, 2003; *Ingrin and Skogby*, 2000; *Bergovici and Karato*, 2003; *Tarits et al*., 2004; *Evans et al*., 2005; *Simpson and Tommasi*, 2005; *Khan and Shankland*, 2012]. In particular, olivine hydration has also been suggested to generate electrical anisotropy due to preferential orientations related to deformation and stress distribution in the lithosphere and the upper asthenosphere [*Evans et al*., 2005; *Simpson and Tommasi*, 2005].

Although this hypothesis has been proposed in 1990 [*Karato*, 1990], the first experimental characterizations of the effect of water on olivine conductivity have been published 16 years later by *Wang et al*. [2006] and *Yoshino et al*. [2006]. Other experimental measurements have completed the data set [*Yoshino et al*., 2009; *Poe et al*., 2010; *Yang*, 2012; *Dai and Karato*, 2014a, 2014b] but the laws derived from these studies predict contrasted conductivities [*Wang et al*., 2006; *Yoshino et al*., 2009; *Poe et al*., 2010; *Jones et al*., 2012], precluding any unequivocal interpretation of electrical conductivities in the upper mantle in terms of mantle hydration (Figure 1a). Much of the debate has focused on the incompatibility of the laws of *Wang et al*. [2006] and *Yoshino et al*. [2009] as they predict the most contrasted conductivities, differing by up to 2 log unit. Indeed, while the former concluded to a strong enhancement of olivine conductivity by minute amounts of water, the latter concluded to a negligible effect at mantle temperatures.

The different groups calibrated their conductivity laws on their own experimental data, probably because of the apparent incompatibility between the different studies. The recent work by *Jones et al*. [2012] was the first attempt of reconciliation. The authors propose a combination of the

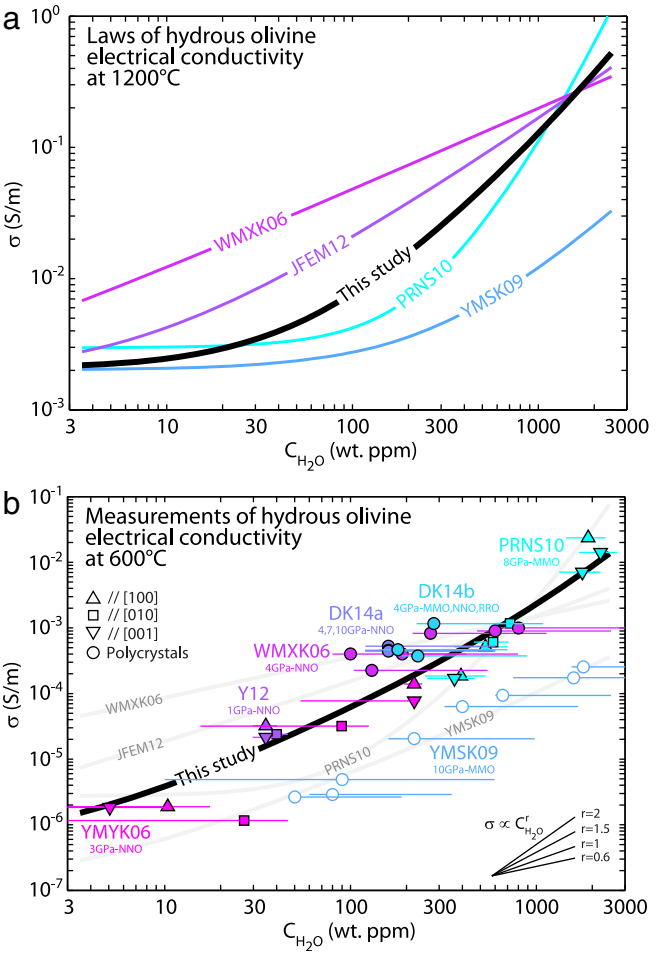

Figure 1. The scatter between the laws of hydrous olivine conductivity versus the consistency of experimental measurements. (a) The contrasting effects of water on olivine conductivity predicted by the existing laws at 1200°C. The black curve is the isotropic conductivity given by our law. (b) The raw experimental conductivity measurements on oriented hydrous olivine single crystals and polycrystals at 600°C (see Appendix A for details on data selection). All of the data follow a single global trend over the whole range of water concentration, which contrasts with all conductivity laws (gray curves) but ours (black curve), except for the ~1 log unit lower conductivities from *Yoshino et al*. [2009]. The horizontal error bars represent the confidence intervals on the water concentration of the samples. The typical ~10–20% uncertainty on conductivity compares with the size of the symbols (not shown). DK14a: *Dai and Karato* [2014a]; DK14b: *Dai and Karato* [2014b]; JFEM12: *Jones et al*. [2012]; PRNS10: *Poe et al*. [2010]; WMXK06: *Wang et al*. [2006]; Y12: *Yang* [2012]; YMSK09: *Yoshino et al*. [2009]; YMYK06: *Yoshino et al*. [2006].

previous laws with a recalibration of some of the key parameters based on conductivity-water content in xenoliths data from the South African craton. The approach by *Jones et al*. [2012] relies on two geophysical observations, and is not based on the analysis of the global experimental database itself.

The inconsistencies between the laboratory studies have essentially been attributed to the various conductivity measurement protocols, however those generally produce uncertainties of about 10–20% only [*Yoshino et al*., 2008, Appendix A]. On the other hand, the concentration of water in the olivine samples are commonly uncertain by several tens of percent and are biased by up to a factor of ~4 when the infrared (IR) calibration of *Paterson* [1982] is used for polycrystals [e.g., *Bell et al*., 2003] (Figure 1b and Appendix Table A1). The concentration of water in olivine is certainly the less well-constrained experimental parameter but was poorly discussed so far, precluding the rigorous test and the whole treatment of the database (note that, in accordance with most studies, the term "water" does not refer to molecular water but to structurally bounded hydrogen (OH groups), which is commonly measured as equivalent H_2O concentration).

Here, we propose that most of the discrepancies between the conductivity laws derive from the experimental uncertainties and biases on the water concentration of the olivine samples. We perform a global analysis of the existing experimental data in order (i) to test the internal consistency of the database and (ii) to adjust a simple empirical law on the largest data set which can be used for geophysical purpose. We propose a new law which calculates the electrical conductivity and anisotropy of olivine as a function of its water content.

2. Consistency of the Experimental Database

The published conductivity measurements on oriented single crystals of hydrous olivine cover wide ranges of water concentration (0–2200 wt ppm) and temperature (200–1440°C) [*Yoshino et al*., 2006; *Poe et al*., 2010; *Yang*, 2012]. The inspection of the run conditions reveals that water content is definitely the experimental parameter having the largest uncertainties, reaching typically several tens of percent (Figure 1b and Appendix Table A1). When these uncertainties are considered, the conductivities collected on single crystals

do form a consistent data set, following a single global trend over the whole range of H_2O concentration (Figure 1b).

The isotropic conductivities collected on hydrous olivine polycrystals by *Wang et al*. [2006] and *Dai and Karato* [2014a, 2014b] also compare fairly well with this trend (Figure 1b). These three studies provide consistent data with values slightly higher than the trend of the oriented single crystal data. This mostly results from the use of the IR calibration of *Paterson* [1982] on olivine polycrystals which is known to underestimate water concentrations by a factor of ∼2–4, depending on the samples and the analytical conditions [*Bell et al*., 2003; *Mosenfelder et al*., 2006a; *Dai and Karato*, 2009; *Withers et al*., 2012]. Up to several tens of percent of hydrogen in the samples of *Wang et al*. [2006] and *Dai and Karato* [2014a, 2014b] is in the form of molecular water, probably in fluid inclusions or in the intergranular medium, as illustrated by the broad band centered at 3400 cm^{-1} superposed to the OH bands on their IR spectra [e.g., *Mosenfelder et al*., 2006b]. Unless this water exsolved from olivine structure during decompression at the end of the runs, it leads to overestimate the concentration of structural hydrogen available for conduction enhancement (note, however, that *Wang et al*. [2006] partially subtracted it; see their Supplementary Information 2). Therefore, the water concentrations of the polycrystals of *Wang et al*. [2006] and *Dai and Karato* [2014a, 2014b] have to be corrected by an unknown factor which may vary from one sample to the other, but which should be less than ∼4. When this additional source of error is considered (right-hand side of the error bars in Figure 1b), the data of *Wang et al*. [2006] and *Dai and Karato* [2014a, 2014b] are undistinguishable from the data obtained on oriented single crystals, and merge with the global trend.

Dai and Karato [2014a, 2014b] investigated the effect of pressure and oxygen fugacity on the conductivity of hydrous olivine. Increasing both parameters decreases conductivity, but to a small extent only. Over the experimental temperature range (600–1000°C), increasing pressure from 4 to 10 GPa and oxygen fugacity from Mo/MoO_2 to Re/ReO_2 buffer decreases conductivity by 0.1–0.3 and 0.3–0.4 log unit, respectively (see also Appendix Figure A1). Note that the change in oxygen fugacity from Mo/MoO_2 to Re/ReO_2 buffer is much greater than the variations expected for the Earth's upper mantle based on petrological surveys [*Frost and McCammon*, 2008]. The effect of pressure on hydrous olivine is similar to that on dry olivine, where conductivity decreases by ∼0.3 log unit from 4 to 10 GPa at 1000°C [*Xu et al*., 2000; *Dai et al*., 2010]. In contrast the effect of oxygen fugacity on hydrous olivine is opposite, since dry olivine conductivity increases by ∼0.4 log unit from Mo/MoO_2 to Ni/NiO buffer at 1000°C [*Dai et al*., 2010]. The change in sign of the oxygen fugacity dependence between dry and hydrous olivine implies that the dependence is weak at intermediate water concentrations (the samples of *Dai and Karato* [2014b] contained 180–280 wt ppm H_2O according to the calibration of *Paterson* [1982]) and even vanishes at a given C_{H2O}. Thus, pressure and oxygen fugacity appears to be parameters of secondary importance, and the electrical conductivity of olivine is mainly correlated to its water content, as can readily be appreciated from the comparison between the various studies (Figure 1b).

The measurements on hydrous olivine polycrystals of *Yoshino et al*. [2009] lay about 1 log unit below the data from the other studies (Figure 1b). Obviously, this gap cannot result from the underestimation of water concentration due to the IR calibration of *Paterson* [1982] as this should shift their data further away from the other studies (Figure 1b). It is not likely attributable to the iron content in their samples (Fo91–92.5) since it is similar to the other studies (Appendix Table A1). As discussed above, it cannot result from differences either in pressure or in oxygen fugacity as these parameters have small effects. For instance, the data of *Yoshino et al*. [2009] are up to almost 2 log unit lower than those of *Poe et al*. [2010] while they were collected at almost the same conditions (10 versus 8 GPa, identical Mo/MoO_2 buffer). The origin of the discrepancy between the data of *Yoshino et al*. [2009] and the rest of the database is unknown: does it result from a different and unidentified experimental condition, or from a bias? It should be mentioned that there is an internal inconsistency in the water contents of the samples reported in their original paper. In their Table 1, the water contents expressed as wt % are, after conversion, ∼10 times higher than those expressed as $H/10^6Si$. Using the water contents expressed in the latter unit shifts their data on the same trend as the others, but the authors recently clarified that the values reported as wt % are the correct ones [*Yoshino et al*., 2014]. Nevertheless, the 50 wt ppm H_2O reported for their driest sample (5K1055) is largely overestimated since no OH bands are visible on the IR spectrum of this sample, while they are clearly apparent on the spectrum of the sample containing ∼100 wt

Table 1. Parameters of the Best Fit Law (Equation (1)) and its Misfits With Experimental Data (Given as Mean Absolute Deviations (MAD) Between the Decimal Logarithm Of Modeled and Experimental Conductivities)[a]

						Calibration of *Bell et al*. [2003]		Calibration of *Withers et al*. [2012]		
Orientation	$\Delta H^{Vacancy}$ (kJ/mol)	$\log \sigma_0^{Vacancy}$ (σ in S/m)	$\Delta H^{Polaron}$ (kJ/mol)	$\log \sigma_0^{Polaron}$ (σ in S/m)	$\Delta H^{Hydrous}$ (kJ/mol)	$\log \sigma_0^{Hydrous}$ (σ in S/m/wt ppm)	α (kJ/mol/wt ppm$^{1/3}$)	$\log \sigma_0^{Hydrous}$ (σ in S/m/wt ppm)	α (kJ/mol/wt ppm$^{1/3}$)	MAD Misfit (log unit)
// [100]	261 ± 48	5.92 ± 1.99	146 ± 27	2.19 ± 1.09	92 ± 9	−1.48 ± 0.57	2.56 ± 0.59	−1.28 ± 0.57	2.99 ± 0.69	0.08
// [010]	268 ± 55	5.45 ± 2.07	141 ± 21	2.38 ± 1.10	95 ± 13	−0.70 ± 0.99	0.88 ± 0.59	−0.51 ± 0.99	1.03 ± 0.69	0.05
// [001]	234 ± 47	4.67 ± 1.94	146 ± 24	2.51 ± 1.06	81 ± 9	−1.97 ± 0.69	1.94 ± 0.54	−1.77 ± 0.69	2.25 ± 0.63	0.06
Isotropic	239 ± 46	5.07 ± 1.32	144 ± 16	2.34 ± 0.67	89 ± 7	−1.37 ± 0.45	1.79 ± 0.47	−1.17 ± 0.45	2.08 ± 0.55	0.10

[a]The overall MAD misfit with the database is 0.07 log unit. Two sets of $\log \sigma_0^{Hydrous}$ and α are reported depending on whether water concentrations from the calibration of *Bell et al*. [2003] or from that of *Withers et al*. [2012] have to be used (the latter law should be preferred when inverting conductivities for obtaining more realistic water concentrations). The isotropic conductivity is reported in the form of equation (1) for sake of simplicity (with a MAD < 0.01 log unit, this fit negligibly deviates from exact geometric average). Errors on individual parameters are given as 2σ (see Figure 3 for uncertainties on predicted isotropic conductivity and conductivity anisotropy).

ppm (5K1223) (see their Figure 2). An overestimation of structural hydrogen due to the integration of molecular water is possible, but it is very unlikely to cause a factor 10 deviation given the amount of molecular water apparent on their IR spectra (see their Figure 2). The issue remains unsolved. Thus, except for the data of *Yoshino et al*. [2009], the conductivity measurements on hydrous olivine are consistent.

3. The New Conductivity Law

Our purpose is to provide a law for geophysical purpose which unifies the largest part of the database. The approach remains empirical since, as we shall see later, the conduction mechanisms in hydrous olivine remain unclear.

We consider the conductivity data from all published experimental measurements on single crystals and polycrystals of hydrous olivine [*Yoshino et al*., 2006; *Wang et al*., 2006; *Poe et al*., 2010; *Yang*, 2012; *Dai and Karato*, 2014a, 2014b]. Additional data from experiments performed under nominally dry conditions are also included to improve accuracy at low water contents and high temperature [*Xu et al*., 2000; *Poe et al*., 2010; *Dai et al*., 2010]. As discussed above, the data of *Yoshino et al*. [2009] are not included, except for the high temperature part (>1400°C) of the measurements on their nominally dry sample (5K1055). The database regroups 287 conductivity measurements on 38 samples with temperatures and water concentrations ranging over 200–1727°C and 0–2200 wt ppm (details on data selection can be found in Appendix A and Table A1).

For the sake of simplicity, pressure and oxygen fugacity dependences are not parameterized since, as mentioned above, the effect of these parameters on the conductivity of olivine appears to be minor compared to that of water concentration. The database compiles experiments performed between 1 and 10 GPa and with Mo/MoO_2 or Ni/NiO buffer in almost equal proportion, so our law is roughly representative of mean upper mantle pressure and oxygen fugacity conditions.

We consider the superposition of three conductive processes

$$\sigma = \sigma_0^{Vacancy}\ e^{-\frac{\Delta H^{Vacancy}}{RT}} + \sigma_0^{Polaron}\ e^{-\frac{\Delta H^{Polaron}}{RT}} + \sigma_0^{Hydrous}\ C_{H2O} e^{-\frac{\Delta H^{Hydrous} - \alpha C_{H2O}^{1/3}}{RT}}, \quad (1)$$

where R is the gas constant, T the absolute temperature, C_{H2O} the concentration of water in olivine, and the σ_0s and the ΔHs the preexponential factors and activation enthalpies, respectively. The two first terms represent electrical conduction in anhydrous olivine, which is controlled by small polaron hopping from ferrous to ferric ions and, at high temperature, by the diffusion of cation vacancies [*Schock et al*., 1989; *Wanamaker and Duba*, 1993; *Xu et al*., 2000; *Constable*, 2006; *Yoshino et al*., 2009; *Dai et al*., 2010]. The third term corresponds to the electrical conduction related to the introduction of hydrogen species. It was applied to conduction in hydrous olivine in order to account, through the positive parameter α, for the decrease of activation enthalpy as a function of water concentration evidenced in the studies where water concentration was varied over wide ranges [*Yoshino et al*., 2006, 2009; *Poe et al*., 2010].

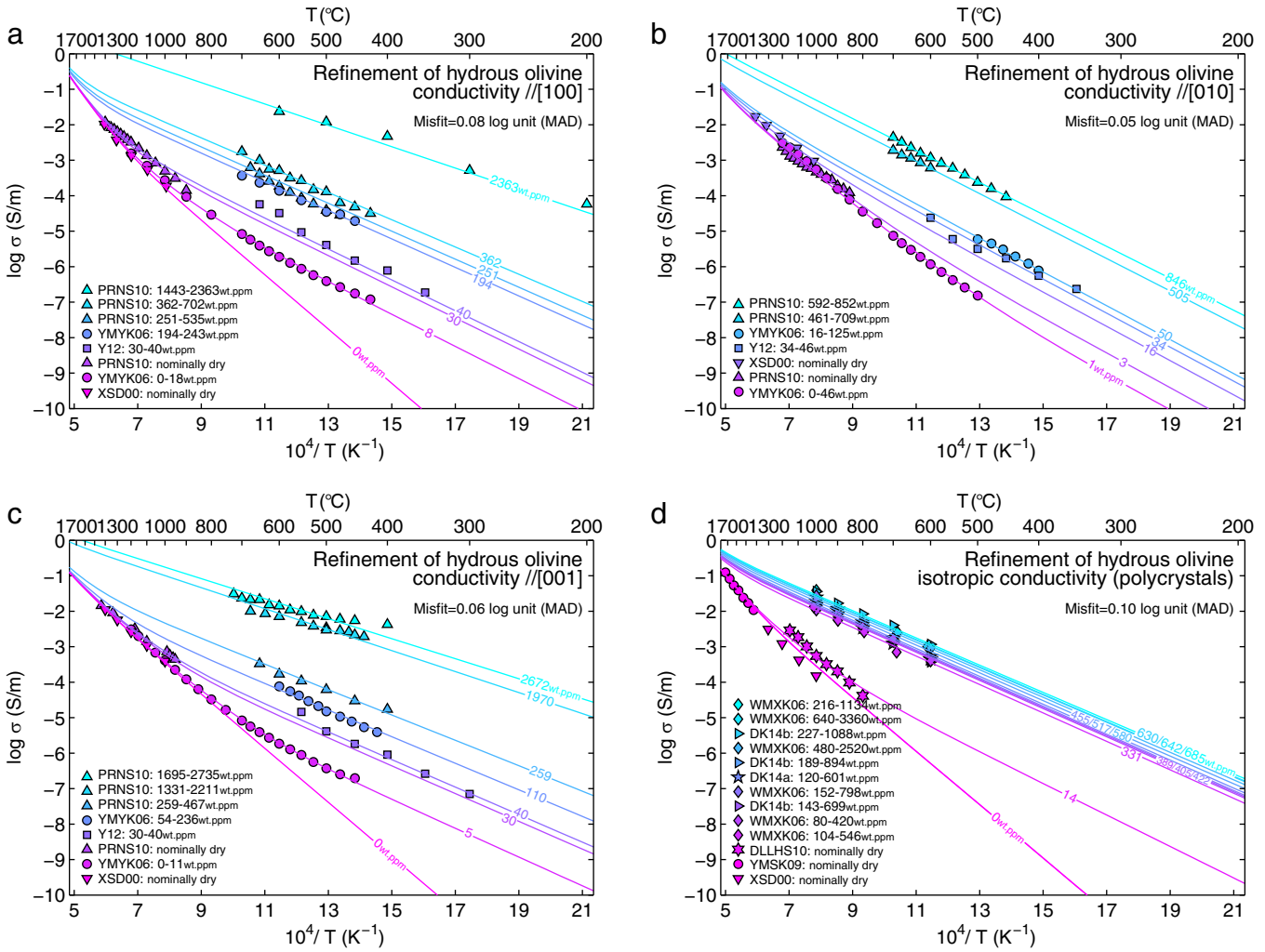

Figure 2. Fit of raw experimental measurements of hydrous olivine conductivity to equation (1). The law is in good agreement with the data acquired along (a) [100], (b) [010], and (c) [001] axes on single crystals, and on (d) polycrystals, with mean absolute deviations (MAD) ranging from 0.05 to 0.10 log unit (the overall MAD with the database is 0.07 log unit). Optimized parameters are reported in Table 1. Water concentrations were allowed to vary within the confidence intervals on the measurements, and optimized values are labeled on the curves (see also Appendix Table A1). DK14a: *Dai and Karato* [2014a]; DK14b: *Dai and Karato* [2014b]; DLLHS10: *Dai et al*. [2010]; PRNS10: *Poe et al*. [2010]; WMXK06: *Wang et al*. [2006]; XSD00: *Xu et al*. [2000]; Y12: *Yang* [2012]; YMSK09: *Yoshino et al*. [2009]; YMYK06: *Yoshino et al*. [2006].

Equation (1) was adjusted on the single crystals data for each of the three axes (σ_{100}, σ_{010}, σ_{001}) along with the geometric mean which was adjusted to polycrystals data

$$\sigma_{\text{Isotropic}} = \sqrt[3]{\sigma_{100}\sigma_{010}\sigma_{001}}. \quad (2)$$

Thus, our law is composed of four equations, i.e., one for each crystallographic axis, allowing addressing conductivity anisotropy, and one for isotropic conductivity, relevant to olivine aggregates without preferential orientation. At each iteration of the optimizing procedure, the three sets of σ_0s, ΔHs, and α from σ_{100}, σ_{010}, and σ_{001} are changed and the geometric mean $\sigma_{\text{Isotropic}}$ is generated, so that the overall misfit with the whole database (mean absolute deviations MAD), from both single crystals and polycrystals, is minimized. The key feature of the modelling is that, for each sample, the water concentration is optimized by allowing it to vary within the confidence intervals on the measurements (see Appendix A and Table A1). The parameters of the fit are therefore interdependent and influenced by all the data. We evaluated the maximum errors the errors on water concentrations (and on experimental conductivities) cause on our law by performing 20,000 fits where water concentrations were not optimized but forced at random values within the confidence intervals (and assuming a 20% random error on conductivities). Errors on individual

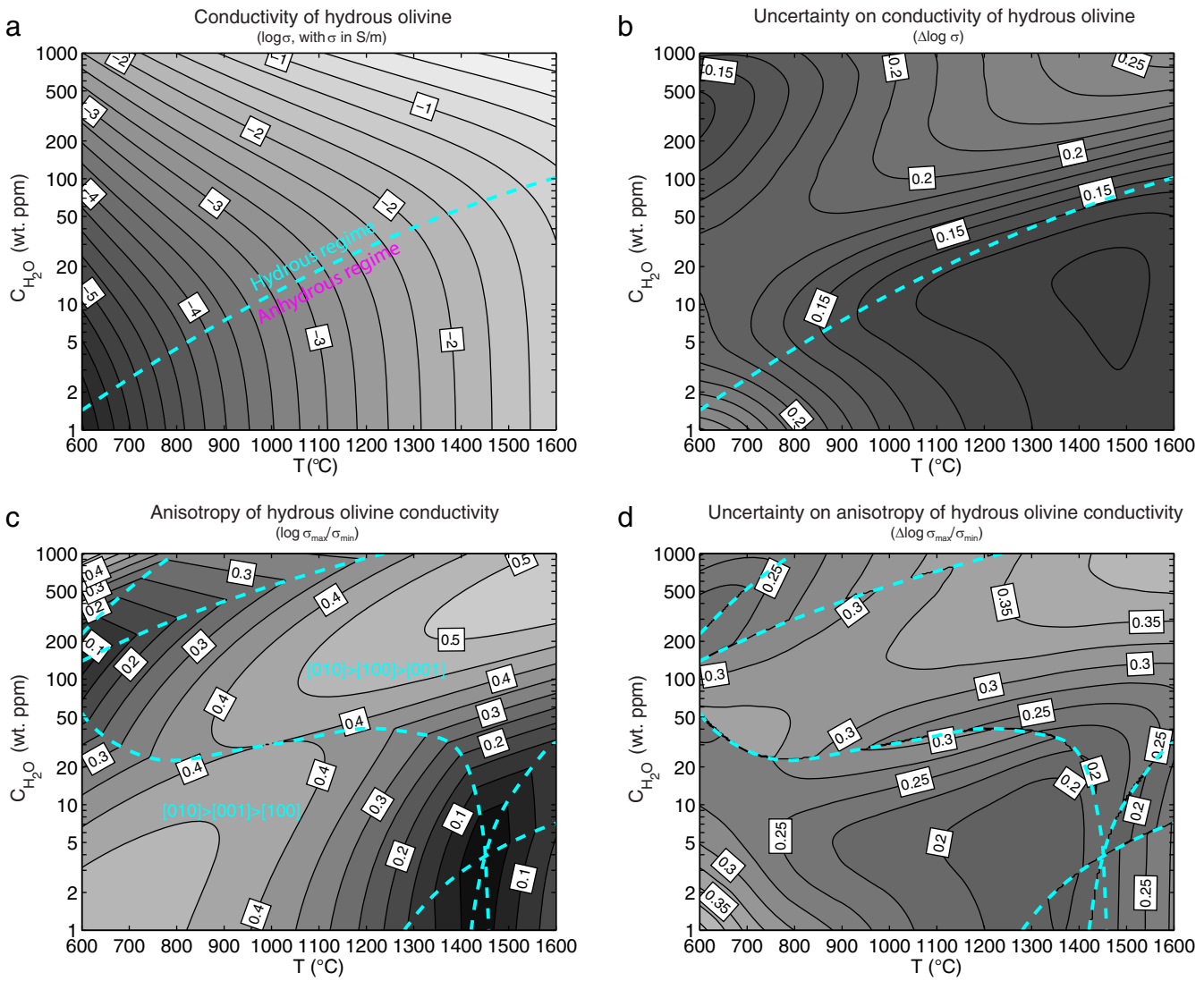

Figure 3. Conductivity and maximum conductivity anisotropy of hydrous olivine according to our law (consistent with the calibration of *Withers et al*. [2012]). (a) Conductivity map (log σ, with σ in S/m) and (b) corresponding uncertainty (2σ) as a function of temperature and water concentration. The dashed curve marks the transition from anhydrous to hydrous regime (equal contribution of anhydrous and hydrous conduction). (c) Maximum conductivity anisotropy map (log $\sigma_{max}/\sigma_{min}$) and (d) corresponding uncertainty (2σ) as a function of temperature and water concentration. The changes in anisotropy orientation are marked by dashed curves.

parameters and on predicted conductivities are calculated as twice the standard deviation of those yielded by the 20,000 simulations.

The results of the best fit law are reported in Figure 2 and in Table 1 (see also Table A1 for optimized water concentrations). The mean absolute deviations with single crystals data are 0.05–0.08 log unit and 0.10 log unit with polycrystals data, corresponding to an overall MAD of 0.07 log unit, which is comparable to the uncertainties on conductivity measurements. The 0.08 and 0.13 log unit MAD with the data acquired at various pressures and oxygen fugacities by *Dai and Karato* [2014a, 2014b], respectively, shows that neglecting these parameters only introduces small biases (Appendix Figure A1). Our optimization yields water contents 2.4 times higher on average than those given by *Wang et al*. [2006] and *Dai and Karato* [2014a, 2014b] for hydrous polycrystals (Appendix Table A1), which falls in the range of correction factors for the calibration of *Paterson* [1982] (i.e., ~2–4) [*Bell et al*., 2003; *Mosenfelder et al*., 2006a; *Dai and Karato*, 2009; *Withers et al*., 2012]. The deviation from the highest correction factors may represent the fraction of hydrogen trapped as molecular water in fluid inclusions which did not contribute to conductivity enhancement. These results confirm that the database is consistent, and is reproduced by a simple law with good accuracy. Including all

the polycrystals data of *Yoshino et al*. [2009] strongly lowers the quality of the fit for both single crystals and polycrystals data, with an overall MAD increased by a factor ~3 (0.23 versus 0.07 log unit; Table A2), confirming that these data for hydrous conduction seem incompatible with the rest of the database.

Withers et al. [2012] reported a new IR calibration which corrects the water concentrations of the calibration of *Bell et al*. [2003] by a factor of ~2/3 (100 wt ppm H_2O according to *Withers et al*. [2012] = 158 wt ppm H_2O according to *Bell et al*. [2003]). As modeled water concentrations are rather consistent with the calibration of *Bell et al*. [2003], we applied this conversion to provide a law consistent with the new calibration of *Withers et al*. [2012] (this changes $\sigma_0^{Hydrous}$ and α only, Table 1). This law should be preferred, especially when inverting conductivities into olivine hydration in order to obtain more realistic water concentrations. Therefore, unless otherwise mentioned, the water concentrations reported below will refer to the calibration of *Withers et al*. [2012]. We still provide a law consistent with the calibration of *Bell et al*. [2003] in order to facilitate comparison with previous works as this calibration was extensively used over the past decade.

The $\Delta H^{Vacancy}$ and $\Delta H^{Polaron}$ values for isotropic conductivity are 239 ± 46 and 144 ± 16 kJ/mol, respectively, in agreement with conduction by small polaron hopping and metal vacancy diffusion in olivine [*Dai et al*., 2010; *Xu et al*., 2000; *Constable*, 2006; *Yoshino et al*., 2009; see also *Chakraborty*, 2010]. The $\Delta H^{Hydrous}$ value is much smaller, i.e., 89 ± 7 kJ/mol for isotropic conductivity, in agreement with previous investigations on hydrous olivine [*Yoshino et al*., 2006; *Wang et al*., 2006; *Yoshino et al*., 2009; *Poe et al*., 2010; *Yang*, 2012; *Dai and Karato*, 2014a, 2014b].

Isotropic conductivity and maximum conductivity anisotropy maps as a function of temperature and water concentration are shown in Figure 3, along with propagated uncertainty maps. As expected, uncertainties are much lower in the domains where measurements were performed than in those where extrapolation is required, for instance, at high temperature and high water concentration (Figure 3). The average uncertainty on the isotropic conductivity is 0.17 log unit over the map (Figure 3b), and is identical in the more mantle-relevant 1000–1500°C and 0–500 wt ppm H_2O range. We noted before that the biases introduced by neglecting the effect of pressure and oxygen fugacity are relatively small, being ~0.1 log unit on average (Appendix Figure A1). Thus, we estimate that the typical error on our law for isotropic conductivity is 0.2–0.3 log unit. The uncertainty on anisotropy is larger and is often comparable to the magnitude of anisotropy, with log $\sigma_{max}/\sigma_{min}$ being 0.34 ± 0.27 over the maps (Figures 3c and 3d). Between 1000 and 1500°C, the mean maximum anisotropy (log $\sigma_{max}/\sigma_{min}$) is 0.21 ± 0.20 for 0–10 wt ppm H_2O, 0.37 ± 0.27 for 10–200 wt ppm H_2O, and 0.46 ± 0.34 for 200–500 wt ppm H_2O. The anisotropy of hydrous olivine might be higher than that of dry olivine, but this is uncertain. In any case, the range of maximum anisotropy including uncertainty indicates that preferential orientation of olivine should produce moderate conductivity anisotropy (~0–0.8 log unit).

4. Comparison With Previous Laws

The law of *Poe et al*. [2010] allows the calculation of both oriented and isotropic conductivities. It yields large MADs when compared with the whole database, being 3 times larger than our law (0.21 versus 0.07 log unit; Table 2). This result is mainly due to the underestimation of the conductivities at intermediate water concentrations since these authors investigated samples with >360 wt ppm H_2O (calibration of *Bell et al*. [2003]), except for nominally dry samples. At 1000 wt ppm H_2O (calibration of *Bell et al*. [2003]) and between 1000 and 1600°C, the law of *Poe et al*. [2010] yields ~1 to 1.3 log unit maximum anisotropy (log $\sigma_{max}/\sigma_{min}$). Even if uncertain, the maximum anisotropy predicted by our law is much lower, being 0.30 ± 0.32 to 0.53 ± 0.38 log unit in the same conditions.

The other published laws provide isotropic conductivities only, so the comparison is restricted to measurements on polycrystals (about one quarter of the database). The MAD of our law with polycrystals data is similar to the law of *Wang et al*. [2006] (0.10 versus 0.11 log unit; Table 2), while most of these data come from their study and those of *Dai and Karato* [2014a, 2014b]. Because *Wang et al*. [2006] underestimated water concentrations with the IR calibration of *Paterson* [1982] and because they did not investigate samples with small water contents (100 wt ppm minimum; calibration of *Paterson* [1982]), their law overestimates the effect of water to more than 1 log unit at water concentrations below ~200 wt ppm (Figure 1b).

The law of *Jones et al*. [2012] has a slightly lower MAD with the polycrystals data (0.09 log unit; Table 2). However, as it is a combination of the previous laws which includes that of *Wang et al*. [2006], it also

Table 2. Characteristics of the Various Laws and Misfits With Experimental Data (Given as Mean Absolute Deviations (MAD) Between the Decimal Logarithm of Modeled and Experimental Conductivities)[a]

						MAD Misfit (log unit) Single Crystals				
Law	Type	Sample Type	Sample #	T (°C)	C_{H_2O} (wt ppm)	// [100]	// [010]	// [001]	Polycrystals	Overall
This study	Isotropic and oriented	Single crystals and polycrystals	38	200–1727	0–2220	0.08	0.05	0.06	0.10	0.07
Poe et al. [2010]	Isotropic and oriented	Single crystals	11	200–1440	360–2220 and nominally dry	0.29	0.28	0.14	0.15	0.21
Jones et al. [2012][b]	Isotropic	Geophysical data[b]	2	740–850	60–150				0.09	
Wang et al. [2006]	Isotropic	Polycrystals	6	600–1000	100–800				0.11	
Yoshino et al. [2009]	Isotropic	Polycrystals	10	500–1727	Nominally dry–1790				0.68	

[a]Following the same procedure as for our law, the MADs between the laws of the other groups and the experimental data were minimized by allowing water concentrations to vary within the confidence intervals. Note that the isotropic laws can only be compared to the polycrystals data, so the MADs are not representative of comparison with the whole database (see section 4). With an overall MAD misfit of 0.07 log unit, our law best reproduces the entire database.

[b]The law of *Jones et al.* [2012] is not based on experimental data but is a combination of the previous laws where some of the key parameters were recalibrated on two mantle conductivity data from the south African craton.

overestimates the conductivities at low to intermediate concentrations, but the overestimation is attenuated (Figure 1b).

The law of *Yoshino et al.* [2009] largely underestimates the conductivities over the whole range of water concentration (0.68 log unit MAD with polycrystals data; Table 2) since it was calibrated on their data. Their law however remains almost parallel to the trend formed by the rest of the database (Figure 1b).

5. Conduction Mechanisms

It is well established that electrical conduction in anhydrous olivine is controlled by small polaron hopping from ferrous to ferric ions and diffusion of metal vacancies [*Schock et al.*, 1989; *Wanamaker and Duba*, 1993; *Xu et al.*, 2000; *Constable*, 2006; *Yoshino et al.*, 2009; *Dai et al.*, 2010]. In contrast, the mechanisms of electrical conduction in hydrous olivine, supposed to be controlled by the diffusion of hydrogen defects, remain unclear. Hydrogen is mainly incorporated as neutral defects in the cationic sublattices of olivine, i.e., as two protons in Me-site vacancies ($(2H)_{Me}^{\times}$ defects) or as four protons at Si site vacancies ($(4H)_{Si}^{\times}$ defects) [e.g., *Bai and Kohlstedt*, 1993; *Braithwaite et al.*, 2003; *Lemaire et al.*, 2004; *Demouchy and Mackwell*, 2006; *Balan et al.*, 2011; *Otsuka and Karato*, 2011; *Ingrin et al.*, 2013]. The diffusion of these defects requires much higher activation energies than electrical conduction in hydrous olivine (~220 and ~450 kJ/mol for $(2H)_{Me}^{\times}$ and $(4H)_{Si}^{\times}$, respectively, versus ~90 kJ/mol) [*Demouchy and Mackwell*, 2006; *Padrón-Navarta et al.*, 2014]. Furthermore, when converted using the Nernst-Einstein equation [e.g., *Philibert*, 1991], the diffusivities of $(2H)_{Me}^{\times}$ and $(4H)_{Si}^{\times}$ yield several order of magnitude lower conductivities (Figure 4). Thus, the diffusion of hydrogen defects in Me and Si sublattices do not control electrical conduction in hydrous olivine. This observation led *S. Karato* and collaborators to propose that conduction is controlled by minor hydrogen defects having much higher mobility, like interstitial protons produced according to the ionization reaction $(2H)_{Me}^{\times} \leftrightarrow H'_{Me} + H_i$ [e.g., *Wang*, 2006; *Karato*, 2013]. This hypothesis is supported by the study of *Dai and Karato* [2014b] where, contrary to dry olivine, hydrous olivine conductivity was found to be negatively correlated to oxygen fugacity. Indeed, the chemistry of hydrogen defects in olivine predicts a dependence of ionized defects concentration on oxygen fugacity under specific electroneutrality conditions [*Huang et al.*, 2005; *Kohlstedt*, 2006]. However, this hypothesis remains incompatible with two major observations.

1. According to defect equilibria, the concentration of interstitial protons, and therefore the conductivity, should be proportional to C_{H2O}^{r}, where the exponent r has to be smaller than $3/4$, depending on the electroneutrality condition [*Huang et al.*, 2005; *Kohlstedt*, 2006]. *Wang et al.* [2006] obtained $r = 0.62$ by fitting their data set as a whole, but this value is uncertain since it is largely scattered when their data are considered one temperature at a time, with r being greater than 1 for the data at 1000°C and even negative for the data at 800 and 900°C (see their Figure 2). Actually, when all the studies are considered, the trend over the whole range of concentrations is not compatible with $r < 3/4$ (Figure 1b). The exponent of the trend is higher than 1 and even increases as a function of water concentration. This increase is in turn fairly well reproduced by the decrease of the activation energy as a function of water concentration from the hydrous term

in equation (1). Note that this decrease requires a broad range of water concentrations to be evidenced, especially at high water concentration, but is rather limited over upper mantle-relevant olivine concentrations (12 kJ/mol from 0 to 200 wt ppm). Tentative fit replacing the hydrous term in equation (1) by the equation (2) of *Wang et al*. [2006], i.e., $\sigma_0^{Hydrous} C_{H2O}^{r} e^{-\frac{\Delta H^{Hydrous}}{RT}}$, is unable to reproduce the database when r is forced to be smaller than $^3/_4$ (overall MAD of 0.22 log unit, Appendix Table A2). Better fits are only obtained when r is free to be greater than 1; the best fit we obtained yields $r = 1.62$ for the isotropic conductivity (Appendix Table A2). It is still less accurate than our law (overall MAD of 0.11 log unit), mainly because it cannot reproduce the decrease of activation energy at high water concentration.

2. To the best of our knowledge, the fastest hydrogen diffusion in olivine was observed during the initial steps of hydration experiments by *Mackwell and Kohlstedt* [1990], *Kohlstedt and Mackwell* [1998], and *Demouchy and Mackwell* [2006]. This fast water incorporation was assumed to occur via the interdiffusive exchange of interstitial proton and polaron, and to be rate-controlled by slower proton diffusion. This mechanism is restricted to minute amounts of water (<5 wt ppm), and further hydrogen incorporation proceeds much more slowly into cation vacancies. However, the fast diffusion of interstitial proton still remains incompatible with the electrical conduction of hydrous olivine since it has a higher activation energy (∼150 versus ∼90 kJ/mol), a much higher and different anisotropy (up to more than 2 log unit, faster along [100] axis) and yields lower conductivity after conversion (Figure 4).

Thus, it is not possible to interpret the electrical conductivity of hydrous olivine in term of hydrogen defects diffusion according to the available data. It could therefore be considered that the electrical conduction of hydrous olivine is rather electronic than ionic, as observed in many hydrogen-doped oxides [*McCluskey et al*., 2012]. Further comprehension of hydrogen diffusion is also required since, for example, it is unclear why the hydrogen-deuterium interdiffusive exchange in olivine [*Du Frane and Tyburczy*, 2012], expected to occur via the fastest mechanisms, is slower than the diffusion of interstitial proton as given by the proton-polaron exchange (Figure 4), and is ∼2 order of magnitude slower in forsterite [*Ingrin and Blanchard*, 2006]. Improved evaluation of hydrous olivine conductivity at high mantle temperatures and high water concentrations requires further measurements in order to detect potential additional mechanisms, but preventing water release from the samples under these conditions is experimentally challenging.

6. Comparison With Geophysical Data and Implications

The recent investigations on two kimberlites fields in southern Africa, namely Jagersfontein on the Kaapvaal craton and Gibeon on the Rehoboth terrane [*Jones et al*., 2012], bring a unique opportunity to test our law against the conductivity of mantle regions where water concentration and temperature are well constrained. Magnetotelluric surveys reported log σ (with σ in S/m) of -3.41 ± 0.41 and -2.78 ± 0.18 at ∼100 km depth, with temperature estimates of 740 ± 25 and 850 ± 25°C for the two locations, respectively [*Jones et al*., 2012]. Based on measurements on xenoliths from the Kaapvaal craton [*Peslier et al*., 2010; *Baptiste et al*., 2012], *Jones et al*. [2012] estimated that the maximum range of water concentration in olivine at ∼100 km beneath Jagersfontein is 60–150 wt ppm (calibration of *Bell et al*. [2003]). They assumed the same range beneath Gibeon. In these settings, our law yields isotropic conductivities (log σ) ranging from -3.92 to -3.20 and from -3.46 to -2.80 for Jagersfontein and Gibeon respectively, which compare very well with the geophysical data. In comparison, the law of *Wang et al*. [2006] requires 8 and 16 wt ppm to reproduce the Jagersfontein and Gibeon conductivities, and more than 800 and 1200 wt ppm for the law of *Yoshino et al*. [2009].

Thus, our law appears to be reliable for cratonic lithosphere and should also be reliable in the other cold regions of the upper mantle, such as the mantle wedge of subduction settings. Similarly to the other laws, it predicts that the enhancement of olivine conductivity by water weakens at high temperature. This is because the contribution of anhydrous conduction increases with temperature and tends to overcome hydrous conduction at high temperature. For instance, adding 500 wt ppm H_2O increases the conductivity by ∼2 log unit at 1000°C, but only by ∼1 log unit at 1500°C (Figure 3a). Above 1300°C, conduction in olivine containing less than 40 wt ppm H_2O is predicted to be dominated by the anhydrous mechanisms (Figure 3a).

We calculated hydrous olivine conductivity profiles along cratonic and oceanic geotherms (Kaapvaal craton from *Jones* [1988], Canadian shield (East Abitibi) from *Jaupart and Mareschal* [1999], 100-Ma oceanic

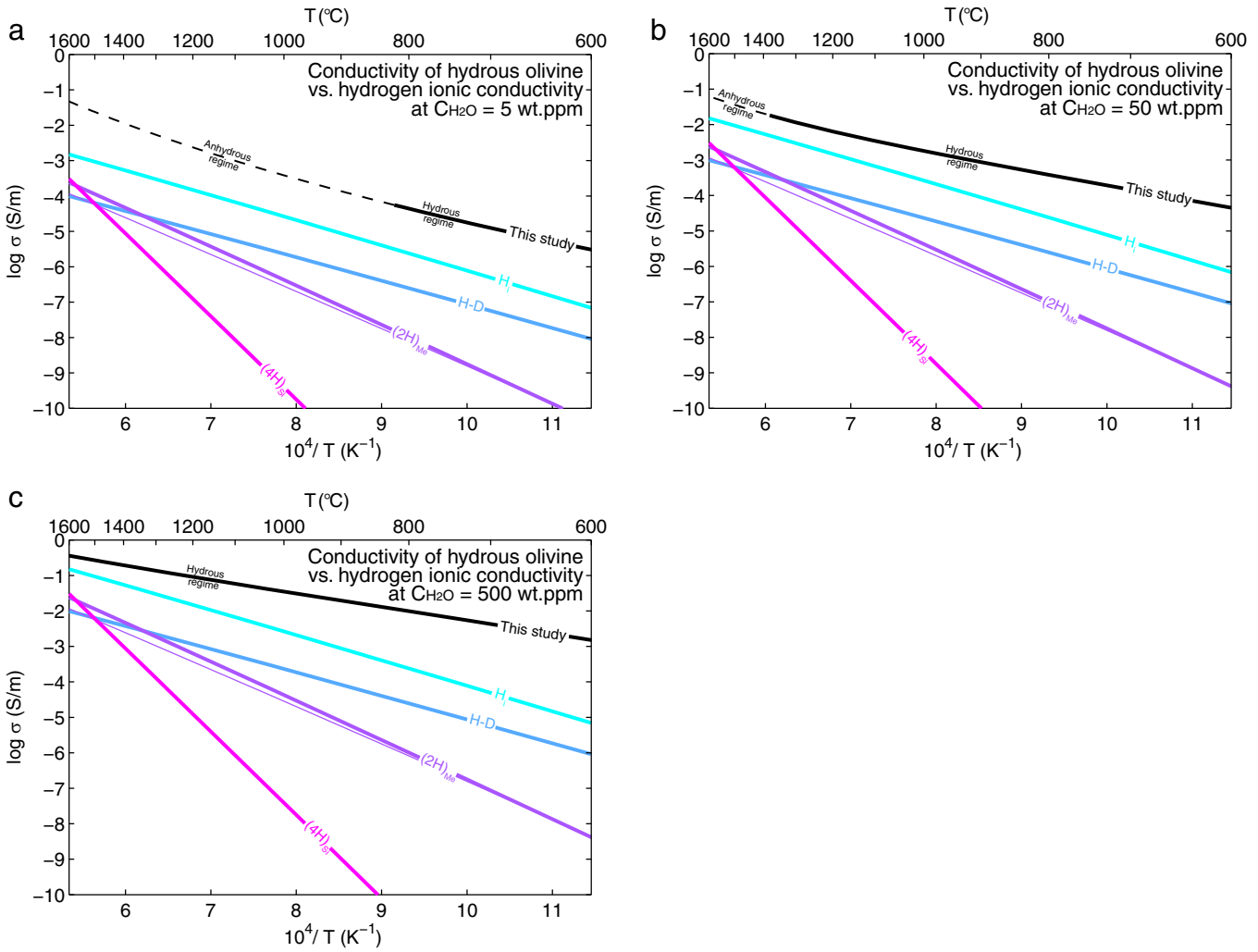

Figure 4. Comparison of the hydrous olivine conductivity law (consistent with the calibration of *Withers et al.* [2012]) to the ionic conductivities of hydrogen defects converted from diffusion data. Calculations were performed using the Nernst-Einstein equation for concentrations of hydrogen defects of (a) 5, (b) 50, and (c) 500 wt ppm H_2O (assuming an olivine density of 3.3 g/cm^3). None of the hydrogen defects mobilities can reproduce the conductivity of hydrous olivine. H_i: interstitial hydrogen-polaron diffusive exchange [*Kohlstedt and Mackwell*, 1998]; H-D: hydrogen-deuterium diffusive exchange [*Du Frane and Tyburczy*, 2012]; $(2H)_{Me}$: diffusion of hydrogen at Me-site (thick line: in-diffusion data of *Demouchy and Mackwell* [2006], thin line: out-diffusion data of *Padrón-Navarta et al.* [2014]); $(4H)_{Me}$: out-diffusion of hydrogen at Si-site [*Padrón-Navarta et al.*, 2014].

lithosphere from *Stixrude and Lithgow-Bertelloni* [2005], ridge adiabat (1600 K potential temperature) from *Stixrude and Lithgow-Bertelloni* [2007], this adiabat was also used at great depths for all the settings; Figure 5). A strong enhancement of conductivity is possible in cratons, for instance ~3 log unit from 0 to 500 wt ppm H_2O at ~100 km depth (Figures 5a and 5b). The enhancement is limited to ~1 log unit from 0 to 500 wt ppm H_2O beneath ridges (Figure 5c). Stronger enhancement is possible in older—and therefore colder—oceanic lithospheres but at shallow depth only since the geotherms converge rapidly to the ridge adiabat (Figure 5c).

The concentration of water in olivine in equilibrium with oceanic mantle is estimated to be 50–200 wt ppm, and ~500 wt ppm maximum at the boundary with the transition zone according to the petrological surveys [*Hirschmann et al.*, 2009; *Ardia et al.*, 2012]. Typical geophysical profiles for cratons and oceans compare fairly well with the conductivities given by our law within this range (Figure 5) [*Baba et al.*, 2010; *Evans et al.*, 2011; *Kuvshinov and Olsen*, 2006; *Lizarralde et al.*, 1995; *Neal et al.*, 2000; *Schultz et al.*, 1993]. Most of the geophysical data are compatible with olivine containing less than 200 wt ppm water, in agreement with petrological predictions. This suggests that the law is also reliable at the highest temperatures of the upper mantle.

It is crucial to consider the geochemical and petrological constraints when interpreting geophysical conductivity data in term of olivine hydration. For example, while the incorporation of ~500 wt ppm H_2O in olivine

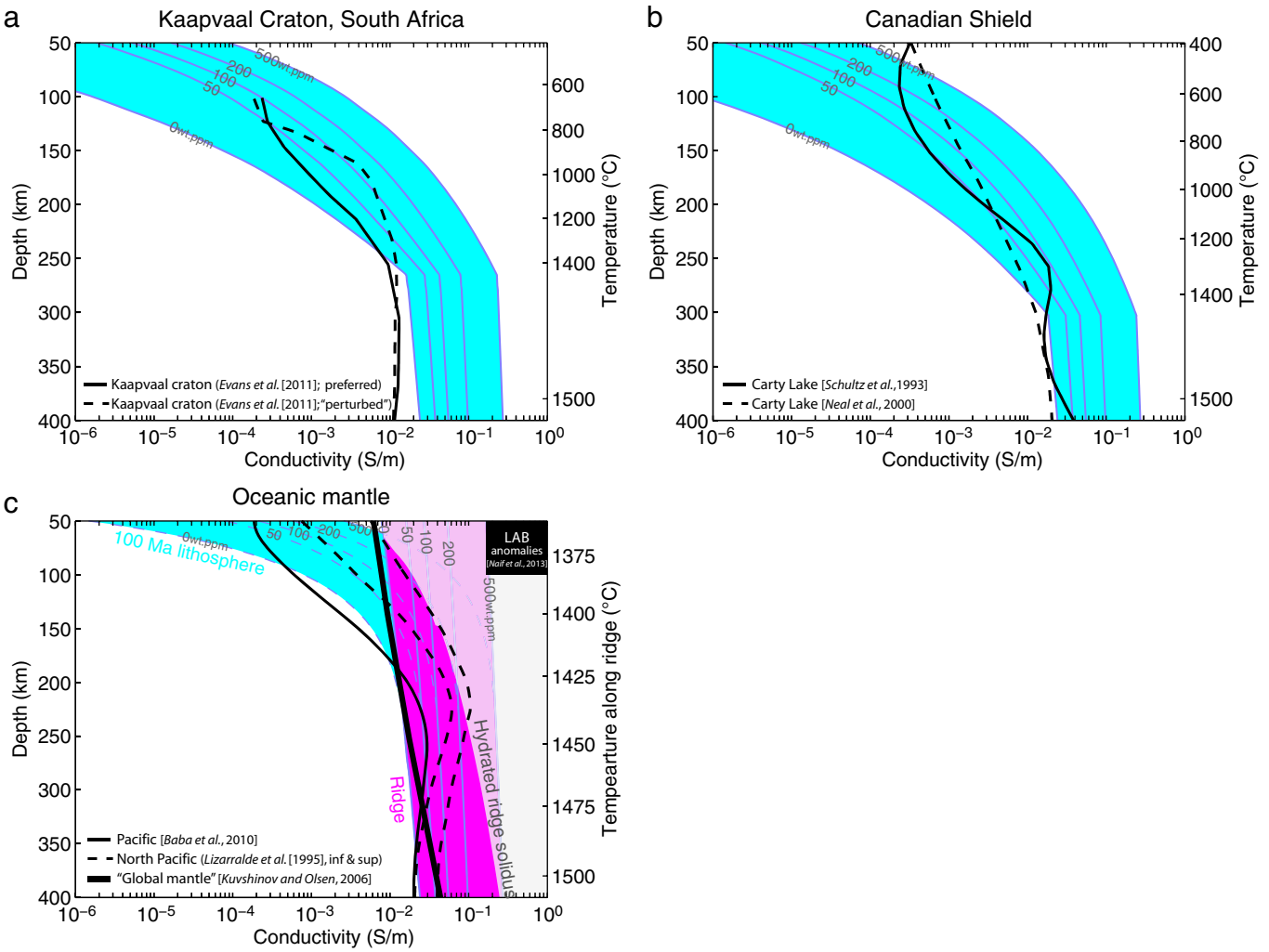

Figure 5. Conductivity of hydrous olivine in (a,b) cratonic and (c) oceanic settings for upper mantle-relevant olivine water concentrations (0–500 w. ppm) according to our law (consistent with the calibration of *Withers et al.* [2012]). Most of the geophysical data are compatible with olivine containing less than 200 wt ppm water, especially at great depth, in line with petrological predictions for normal mantle hydration. The gray transparent area in (c) corresponds to conductivities which require water concentrations higher than the storage capacity of olivine in equilibrium with peridotite along a ridge adiabat, i.e., the region where dehydration melting occurs. High conductivities (>0.1 S/m) in melt-free mantle can thus be reached at high depth only (>250 km and >200 wt ppm H_2O). See section 6 for references and calculation details.

is possible at 400 km depth, it is limited to ∼200 wt ppm at 200 km and ∼50 wt ppm at 100 km beneath young oceanic lithospheres [*Hirschmann et al.*, 2009; *Ardia et al.*, 2012]. We calculated the conductivity at the water storage capacity of olivine equilibrated in bulk rock peridotite along a ridge adiabat, that is the maximum conductivity of hydrous olivine before the onset of peridotite melting (Figure 5c; data from *Hirschmann et al.* [2009] for $P < 5$ GPa (∼150 km) and from *Ardia et al.* [2012] for $P > 5$ GPa). Above this limit, the conductivities are strongly modified since partial melts are present and water is redistributed from olivine to the liquid phase [see *Naif et al.*, 2013; *Sifré et al.*, 2014]. Although higher water storage is allowed in colder settings, the conductivities remain always lower than those beneath ridges because of the decrease in temperature (Figure 5). Thus, water-induced high conductivities in melt-free mantle are predicted at great depth and high water concentration only, for instance 0.1 S/m at more than 250 km and 200 wt ppm in olivine (Figure 5). The high conductivity values observed at the vicinity of the lithosphere-asthenosphere boundary [e.g., *Naif et al.*, 2013] cannot be explained by olivine hydration (Figure 5c). Conductivities of 0.1 S/m or more at 50–100 km depth requires >300 wt ppm H_2O in olivine, implying >1000–1500 wt ppm H_2O in an equilibrated bulk rock peridotite, which is well above the ∼0–200 wt ppm at which peridotite starts melting at these depths [*Hirschmann et al.*, 2009]. On the other hand, these high conductivities are compatible with incipient melting of the mantle, producing highly conductive CO_2-H_2O rich melts [*Yoshino*

Table A1. Run Conditions of the Experimental Studies, With Measured and Modeled Water Concentration in the Olivine Samples (the Ranges in Parentheses are the Confidence Intervals in Which Water Concentration was Allowed to Vary for Optimization)

							C_{H_2O} (wt ppm)	
Sample	Reference	Run#	Mg#	P (GPa)	O_2 Buffer	FTIR/Calibration	Measured	Modeled
Single crystal // [100]	*Poe et al.* [2010]	H2329	90	8	Mo/MoO_2	None	Nominally dry (0–30)	30
		H2474				Polarized/*Bell et al.* [2003]	393 (251–535)	251
		H2473					532 (362–702)	362
		H2320					1903 (1443–2363)	2363
	Xu et al. [2000]	H811	90	4[b]	Mo/MoO_2	None	Nominally dry (0–30)	0
	Yang [2012]	n.c.	91	1	Ni/NiO	Polarized/*Bell et al.* [2003]	35 (30–40)	40
	Yoshino et al. [2006]	1K520	92	3	Ni/NiO	Unpolarized/*Paterson* [1982]	10 (0–18)	8
		1K471					220 (194–243)	194
Single crystal // [010]	*Poe et al.* [2010]	H2476	90	8	Mo/MoO_2	None	Nominally dry (0–30)	3
		H2480				Polarized/*Bell et al.* [2003]	585 (461–709)	505
		H2477					722 (592–852)	846
	Xu et al. [2000]	2013	90	4[b]	Mo/MoO_2	None	Nominally dry (0–30)	16
	Yang [2012]	n.c.	91	1	Ni/NiO	Polarized/*Bell et al.* [2003]	40 (34–46)	34
	Yoshino et al. [2006]	1K524	92	3	Ni/NiO	Unpolarized/*Paterson* [1982]	27 (0–46)	1
		1K482					90 (16–125)	50
Single crystal // [001]	*Poe et al.* [2010]	H2328	90	8	Mo/MoO_2	None	Nominally dry (0–30)	30
		H2472				Polarized/*Bell et al.* [2003]	363 (259–467)	259
		H2324					1771 (1331–2211)	1970
		S3740					2215 (1695–2735)	2672
	Xu et al. [2000]	H820	90	4[b]	Mo/MoO_2	None	Nominally dry (0–30)	0
	Yang [2012]	n.c.	91	1	Ni/NiO	Polarized/*Bell et al.* [2003]	35 (30–40)	40
	Yoshino et al. [2006]	1K521	92	3	Ni/NiO	Unpolarized/*Paterson* [1982]	5 (0–11)	5
		1K478					220 (54–236)	110
Polycrystal (isotropic)	*Dai et al.* [2010]	n.c.	SC[a]	4[b]	Mo/MoO_2	None	Nominally dry (0–30)	14
	Dai and Karato [2014a]	K1318	SC[a]	4	Ni/NiO	Unpolarized/*Paterson* [1982]	160 (120–601)	455
		K1321		7			160 (120–601)	455
		K1323		10			160 (120–601)	455
	Dai and Karato [2014b]	K1398	SC[a]	4	Ni/NiO	Unpolarized/*Paterson* [1982]	180 (143–699)	405
		K1403			Re/ReO_2		230 (189–894)	517
		K1400			Mo/MoO_2		280 (227–1088)	630
	Wang et al. [2006]	K500	SC[a]	4	Ni/NiO	Unpolarized/*Paterson* [1982]	100 (80–420)	389
		K492					130 (104–546)	331
		K488					190 (152–798)	422
		K428					270 (216–1134)	685
		K468					600 (480–2520)	580
		K462					800 (640–3360)	642
	Xu et al. [2000]	H813	90	4[b]	Mo/MoO_2	None	Nominally dry (0–30)	0
	Yoshino et al. [2009]	5K1055	91	10	Mo/MoO_2	Unpolarized/*Paterson* [1982]	Nominally dry (0–30)	0

[a]San Carlos olivine. Mg# not communicated.
[b]Various pressures were investigated by *Xu et al.* [2000] and *Dai et al.* [2010] on their nominally dry samples. 4 GPa was chosen as intermediate value.

et al., 2010; *Sifré et al.*, 2014]. Thus, the enhancement of olivine conductivity by water over mantle-relevant water concentrations can reproduce the range of normal upper mantle conductivities, but appears unlikely to produce the highest conductivities of the upper mantle.

7. Conclusions

The analysis of the measurements of hydrous olivine conductivity shows that the experimental data from laboratory studies are mostly consistent when the uncertainties and biases in the water contents of the olivine samples are considered. Our new law of hydrous olivine conductivity best reproduces the experimental database, and is compatible with most of geophysical data within petrological constraints on mantle hydration. Nevertheless, the mechanism of olivine conductivity enhancement by water remains to be determined, as it appears incompatible with the diffusion of any hydrogen defects according to the literature data. New conductivity measurements at the highest mantle-relevant temperatures and water concentrations would also be desirable, even though those are experimentally challenging.

Table A2. Results of Alternative Fits[a]

		Law			
Orientation	Parameter	Equation (1) Including All data of *Yoshino et al.* [2009]	Equation (1) With *Wang et al.*'s [2006] equation (2) as Hydrous Term: Forcing $r < 0.75$	Equation (1) With *Wang et al.*'s [2006] equation (2) as Hydrous Term: r Unconstrained	Our Best Fit Law (equation (1))
// [100]	$\log \sigma_0^{Vacancy}$ (σ in S/m)	4.73	5.39	5.39	5.92
	$\Delta H^{Vacancy}$ (kJ/mol)	226	241	241	261
	$\log \sigma_0^{Polaron}$ (σ in S/m)	1.89	1.55	1.68	2.19
	$\Delta H^{Polaron}$ (kJ/mol)	135	128	128	146
	$\log \sigma_0^{Hydrous}$	−2.29	−1.35	−4.36	−1.48
	$\Delta H^{Hydrous}$ (kJ/mol)	81	67	66	92
	α (kJ/mol/wt ppm$^{1/3}$)	1.85			2.56
	r		0.75	1.99	
	MAD Misfit (log unit)	0.19	0.25	0.15	0.08
// [010]	$\log \sigma_0^{Vacancy}$ (σ in S/m)	4.51	4.94	3.84	5.45
	$\Delta H^{Vacancy}$ (kJ/mol)	244	237	234	268
	$\log \sigma_0^{Polaron}$ (σ in S/m)	2.55	1.89	2.49	2.38
	$\Delta H^{Polaron}$ (kJ/mol)	147	130	145	141
	$\log \sigma_0^{Hydrous}$	−0.87	0.77	−0.18	−0.70
	$\Delta H^{Hydrous}$ (kJ/mol)	96	102	103	95
	α (kJ/mol/wt ppm$^{1/3}$)	0.42			0.88
	r		0.75	1.17	
	MAD Misfit (log unit)	0.19	0.12	0.08	0.05
// [001]	$\log \sigma_0^{Vacancy}$ (σ in S/m)	3.68	5.01	4.80	4.67
	$\Delta H^{Vacancy}$ (kJ/mol)	240	248	230	234
	$\log \sigma_0^{Polaron}$ (σ in S/m)	2.81	2.51	2.16	2.51
	$\Delta H^{Polaron}$ (kJ/mol)	154	146	136	146
	$\log \sigma_0^{Hydrous}$	−1.90	−0.59	−4.27	−1.97
	$\Delta H^{Hydrous}$ (kJ/mol)	87	73	61	81
	α (kJ/mol/wt ppm$^{1/3}$)	2.12			1.94
	r		0.75	1.79	
	MAD Misfit (log unit)	0.15	0.36	0.10	0.06
Isotropic	$\log \sigma_0^{Vacancy}$ (σ in S/m)	4.45	5.12	4.97	5.07
	$\Delta H^{Vacancy}$ (kJ/mol)	228	238	235	239
	$\log \sigma_0^{Polaron}$ (σ in S/m)	2.42	1.99	2.16	2.34
	$\Delta H^{Polaron}$ (kJ/mol)	146	135	137	144
	$\log \sigma_0^{Hydrous}$	−1.68	−0.37	−2.80	−1.37
	$\Delta H^{Hydrous}$ (kJ/mol)	88	81	77	89
	α (kJ/mol/wt ppm$^{1/3}$)	1.46			1.79
	r		0.75	1.62	
	MAD Misfit (log unit)	0.31	0.11	0.11	0.10
Overall MAD misfit (log unit)		0.23	0.22	0.11	0.07

[a](i) Fit with equation (1) but including all the data of *Yoshino et al.* [2009] to the database. The quality of the fit is strongly decreased. (ii) The hydrous term in equation (1) is replaced by equation (2) from *Wang et al.* [2006], i.e., $\sigma_0^{Hydrous} C_{H_2O}^r e^{-\frac{\Delta H^{Hydrous}}{RT}}$, where the exponent r is forced to be smaller than 0.75. It is unable to reproduce the data. The refinements are fixed at bound $r = 0.75$ but tend to higher values. (iii) Same without constraints on r. Better fits are all obtained for $r > 1$, but they are still less accurate than our law. (iv) Our best fit law (equation (1)) for comparison. Misfits are reported as mean absolute deviations (MAD) between the decimal logarithm of modeled and experimental conductivities.

Our law predicts that the enhancement of olivine conductivity by water is limited to ~1 log unit beneath young oceanic lithospheres for mantle-relevant olivine concentrations (0–500 wt ppm H_2O). Strongest enhancements are expected in the coldest regions of the upper mantle, such as cratonic lithospheres and the mantle wedge of subduction settings. Conductivity anisotropy of hydrous olivine is uncertain. It might be more than dry olivine, but is limited to ~0.8 log unit at most. Therefore, preferential orientation of olivine should produce moderate anisotropy. High conductivities in melt-free mantle can be obtained at great depth and high water concentration only (0.1 S/m requires more than 250 km depth and 200 wt ppm H_2O). The hydration of olivine thus appears unlikely to produce the highest conductivities of the upper mantle.

Appendix A: Details on Data Selection and Modeling

The conductivities of hydrous olivine oriented single crystals and polycrystals used to calibrate our law are raw experimental data as reported in the original papers, apart from the following exceptions. (i) When repeated, measurements at given temperature and water concentration were averaged. (ii) The [001]

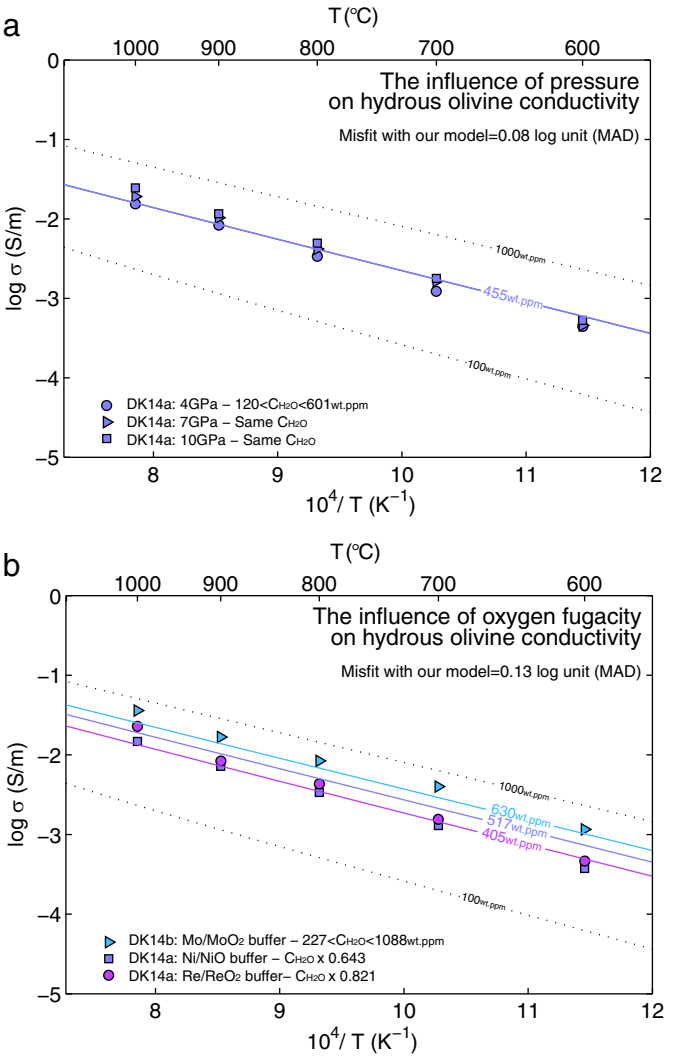

Figure A1. The influence of (a) pressure and (b) oxygen fugacity on the electrical conductivity of hydrous olivine (data acquired on polycrystals by *Dai and Karato* [2014a, 2014b], respectively). These parameters have a weak influence on the electrical conductivity of hydrous olivine compared to that of water, as illustrated by the small dispersion of the data around our adjustments (these data were included in our global treatment; (a) and (b) were extracted from Figure 2d). Note that in order to avoid the effects of pressure and oxygen fugacity to be adjusted by optimizing water concentrations, the measurements at 4, 7, and 10 GPa of *Dai and Karato* [2014a] were modeled imposing the same water concentration in the three cases, and the measurements using Mo/MoO_2, Ni/NiO, and Re/ReO_2 oxygen buffers of *Dai and Karato* [2014b] were modeled imposing constant ratios among the three water concentrations (see Text in Appendix A).

measurements of *Xu et al*. [2000] on nominally dry olivine were generated from their Arrhenius law. (iii) In order to highlight the influence of oxygen fugacity, *Dai and Karato* [2014b] normalized their conductivities to the same water concentration assuming $\sigma \propto C_{H2O}^{r}$ with $r = 0.62$. We obtained their raw conductivities by applying the reverse operation. (iv) The three data points corresponding to the measurements at the highest temperature for each of the three axes of *Yang* [2012] were dismissed since artificially high due to a higher contribution from the assembly background conduction and/or sample dehydration at these temperatures, as mentioned by the author.

Raw data were also reported in Figure 1b, except for the 90 wt ppm [010] measurement from *Yoshino et al*. [2006] which was extrapolated at 600°C from $T < 500$°C, the measurements of *Wang et al*. [2006] at 130 and 270 wt ppm which were extrapolated at 600°C from $T > 700$°C. The conductivities of *Yoshino et al*. [2009] were interpolated at 600°C, except for the measurement at 220 wt ppm which is raw datum and the measurement at 400 wt ppm which was extrapolated from $T < 527$°C. A temperature of 600°C was chosen for this figure as it is the highest experimental temperature at which raw data from all studies can be compared over the widest range of water concentration with minimum extrapolations.

The confidence intervals on water concentrations in which optimization was allowed were those reported in the experimental studies, assuming nonetheless a minimum uncertainty of 15% (Table A1). For the nominally dry samples where water concentration was not measured [*Xu et al*., 2000; *Dai et al*., 2010; *Poe et al*., 2010], we considered 0–30 wt ppm as plausible range since initially dry samples may uptake up to a few tens of wt ppm water in high pressure devices [*Yoshino et al*., 2006]. As discussed in section 2, the upper limits of the confidence intervals on the water concentration of the polycrytals were multiplied by a factor of 3.5 according to *Bell et al*. [2003], resulting in upper limits about ~4 times higher than the mean values reported by *Wang et al*. [2006] and *Dai and Karato* [2014a, 2014b] with the calibration of *Paterson* [1982] (Table A1). Some additional constraints were imposed on the modelling of the data of *Dai and Karato* [2014a, 2014b] in order to avoid the effects of pressure and oxygen fugacity to be adjusted by optimizing water concentrations and therefore to evaluate the biases introduced by the law when these parameters

are varied. The measurements at 4, 7, and 10 GPa of *Dai and Karato* [2014a] were performed on samples containing the same water concentration, therefore we imposed the water concentrations to be the same in the three samples. The measurements using Mo/MoO_2, Ni/NiO, and Re/ReO_2 oxygen buffers of *Dai and Karato* [2014b] were obtained on samples containing different amount of water, therefore we imposed the ratios among the water concentration of the three samples to be constant.

Single frequency conductivity measurements, as those of *Yoshino et al*. [2006], have been argued to introduce biases. However, those modify the conductivities by 10–20% only [*Yoshino et al*., 2008]. This is negligible in front of the uncertainties on water concentrations, and actually compares with the size of the symbols in Figure 1b. It also has been argued that the conductivities of *Poe et al*. [2010] might be artificially high due to the release of water during their runs. However, the release of water would have irrevocably led to a gap in the conductivities and it is clear from Figure 1b that their data form a single trend with the others. An important part of the OH bands in the IR spectra of the olivine hydrated at 0.2 GPa by *Yang* [2012] are found at low wave number ($<$3400 cm^{-1}). These bands are typical of low pressure hydrous olivine [*Withers et al*., 2012; *Ingrin et al*., 2013], and are mostly absent in the other studies where hydrations were performed at much higher pressures (several GPa). *Bell et al*. [2003] mentioned that the application of their calibration to these bands could overestimate the OH content, but this remains to be verified experimentally. The water contents reported by *Yang* [2012] might therefore be overestimated, but his data can be satisfactorily modeled within reported confidence intervals on C_{H_2O} (Figure 2). The magnitude of the dependence of hydrous olivine conductivity on oxygen fugacity reported by *Dai and Karato* [2014b] might be modified if the water concentrations of their samples were recalculated removing molecular water and considering the sole OH bands. Nevertheless, it is clear from the comparison of the various studies that the effect of oxygen fugacity is weak and minor compared to that of water (Figure 1b).

Acknowledgments

We are grateful to Alan G. Jones and two anonymous reviewers who greatly contributed to improve our analysis and our conductivity law. We also acknowledge the efficient editorial handling by Thorsten W. Becker. The data for this paper are from published articles as referenced in the Text and in Appendix A. This work, part of the ElectroLith project, benefited from funding by the European Research Council (ERC project 279790) and the French agency for research (ANR project 2010 BLAN 621 01).

References

Ardia, P., M. M. Hirschmann, A. C. Withers, and T. J. Tenneri (2012), H_2O storage capacity of olivine at 5–8 GPa and consequences for dehydration partial melting of the upper mantle, *Earth Planet. Sci. Lett.*, *345–348*, 104–116.

Baba, K., H. Utada, T. N. Goto, T. Kasaya, H. Shimizu, and N. Tada (2010), Electrical conductivity imaging of the Philippine Sea upper mantle using seafloor magnetotelluric data, *Phys. Earth Planet. Inter.*, *183*, 44–62.

Bai, Q., and D. L. Kohlstedt (1993), Substantial hydrogen solubility in olivine and implications for water storage in the mantle, *Nature*, *357*, 672–674.

Balan, E., J. Ingrin, S. Delattre, I. Kovacs, and M. Blanchard (2011), Theoretical infrared spectrum of OH-defects in forsterite, *Eur. J. Mineral.*, *23*(3), 285–292.

Baptiste, V., A. Tommasi, and S. Demouchy (2012), Deformation and hydration of the lithospheric mantle beneath the Kaapvaal craton, South Africa, *Lithos*, *149*, 31–50.

Bell, D. R., G. R. Rossman, J. Maldener, D. Endisch, and F. Rauch (2003), Hydroxide in olivine: A quantitative determination of the absolute amount and calibration of the IR spectrum, *J. Geophys. Res.*, *108*(B2), 2105, doi:10.1029/2001JB000679.

Bercovici, D., and S. Karato (2003), Whole-mantle convection and transition-zone water filter, *Nature*, *425*, 39–44.

Braithwaite, J. S., K. Wright, and C. R. A. Catlow (2003), A theoretical study of the energetics and IR frequencies of hydroxyl defects in forsterite, *J. Geophys. Res.*, *108*(B6), 2284, doi:10.1029/2002JB002126.

Chakraborty, S. (2010), Diffusion coefficients in olivine, wadsleyite and ringwoodite, *Rev. Miner. Geochem.*, *72*, 603–639.

Constable, S. (2006), SEO3: A new model of olivine electrical conductivity, *Geophys. J. Int.*, *166*, 435–437.

Dai, L., and S. Karato (2009), Electrical conductivity of orthopyroxene: Implications for the water content of the asthenosphere, *Proc. Jpn. Acad., Ser. B*, *85*, 466–475, doi:10.2183/pjab.85.466.

Dai, L., and S. Karato (2014a), The effect of pressure on the electrical conductivity of olivine under the hydrogen-rich conditions, *Phys. Earth Planet. Inter.*, *232*, 51–56.

Dai, L., and S. Karato (2014b), Influence of oxygen fugacity on the electrical conductivity of olivine: Implications for the mechanism of conduction, *Phys. Earth Planet. Inter.*, *232*, 57–60.

Dai, L., H. Li, C. Li, H. Hu, and S. Shan (2010), The electrical conductivity of dry polycrystalline olivine compacts at high temperatures and pressures, *Mineral. Mag.*, *74*, 849–857.

Demouchy, S., and S. J. Mackwell (2006), Mechanisms of hydrogen incorporation and diffusion in iron-bearing olivine, *Phys. Chem. Miner.*, *33*, 347–355.

Du Frane, W. L., and J. A. Tyburczy (2012), Deuterium-hydrogen exchange in olivine: Implications for point defects and electrical conductivity, *Geochem. Geophys. Geosyst.*, *13*, Q03004, doi:10.1029/2011GC003895.

Evans, R. L., G. Hirth, K. Baba, D. W. Forsyth, A. Chave, and R. Makie (2005), Geophysical evidence from the MELT area for compositional control on oceanic plates, *Nature*, *437*, 249–252.

Evans, R. L., et al. (2011), Electrical lithosphere beneath the Kaapvaal craton, southern Africa, *J. Geophys. Res.*, *116*, B04105, doi:10.1029/2010JB007883.

Frost, D. J., and C. A. McCammon (2008), The redox state of Earth's mantle, *Annu. Rev. Earth Sci.*, *36*, 249–252.

Hirschmann, M. M., T. Tenner, C. Aubaud, and A. C. Withers (2009), Dehydration melting of nominally anhydrous mantle: The primacy of partitioning, *Phys. Earth Planet. Inter.*, *176*, 54–68.

Hirth, G., and D. L. Kohlstedt (1996), Water in the oceanic upper mantle: Implications for rheology, melt extraction and the evolution of the lithosphere, *Earth Planet. Sci. Lett.*, *144*, 93–108.

Hirth, G., and D. L. Kohlstedt (2003), Rheology of the upper mantle and the mantle wedge: A view from the experimentalists, in *Inside the Subduction Factory, Geophys. Monogr. Ser.*, vol. 138, edited by J. Eiler, pp. 83–105, AGU, Washington, D. C.

Huang, X., X. Yousheng, and S. Karato (2005), Water content in the transition zone from electrical conductivity of wadsleyite and ringwoodite, *Nature*, *434*, 746–749.
Ingrin, J., and M. Blanchard (2006), Diffusion of hydrogen in minerals, *Rev. Miner. Geochem.*, *62*, 291–320.
Ingrin, J., and H. Skogby (2000), Hydrogen in nominally anhydrous upper-mantle minerals: Concentration levels and implications, *Eur. J. Mineral.*, *12*, 543–570.
Ingrin, J., J. Liu, C. Depecker, S. C. Kohn, E. Balan, and K. J. Grant (2013), Low-temperature evolution of OH bands in synthetic forsterite, implication for the nature of H defects at high pressure, *Phys. Chem. Miner.*, *40*, 499–510.
Jaupart, C., and J. C. Mareschal (1999), The thermal structure and thickness of continental roots, *Lithos*, *48*, 93–114.
Jones, A. G., J. Fullea, R. L. Evans, and M. R. Muller (2012), Water in cratonic lithosphere: Calibrating laboratory determined models of electrical conductivity of mantle minerals using geophysical and petrological observations, *Geochem. Geophys. Geosyst.*, *13*, Q06010, doi: 10.1029/2012GC004055.
Jones, M. Q. W. (1988), Heat Flow in the Witwatersrand Basin and environs and its significance for the south African shield geotherm and lithosphere thickness, *J. Geophys. Res.*, *93*(B4), 3243–3260.
Karato, S. (1990), The role of hydrogen in the electrical conductivity of the upper mantle, *Nature*, *347*, 272–273.
Karato, S. (2013), Theory of isotope diffusion in a material with multiple species and its implications for hydrogen-enhanced electrical conductivity in olivine, *Phys. Earth Planet. Inter.*, *219*, 49–54.
Khan, A., and T. J. A. Shankland (2012), Geophysical perspective on mantle water content and melting: Inverting electromagnetic sounding data using laboratory-based electrical conductivity profiles, *Earth Planet. Sci. Lett.*, *317–318*, 27–43.
Kohlstedt, D. L. (2006), The role of water in high-temperature rock deformation, *Rev. Miner. Geochem.*, *62*, 377–396.
Kohlstedt, D. L., and S. J. Mackwell (1998), Diffusion of hydrogen and intrinsic point defects in olivine, *Z. Phys. Chem.*, *207*, 147–162.
Kuvshinov, A., and N. Olsen (2006), A global model of mantle conductivity derived from 5 years of CHAMP, Ørsted, and SAC-C magnetic data, *Geophys. Rev. Lett.*, *33*, L18301, doi:10.1029/2006GL027083.
Lemaire C., S. C. Kohn, and R. A. Brooker (2004), The effect of silica activity on the incorporation mechanism of water in synthetic forsterite: A polarised infrared spectroscopic study, *Contrib. Mineral. Petrol.*, *147*, 48–57.
Lizarralde, D., A. Chave, G. Hirth, and A. Schultz (1995), Northeastern Pacific mantle conductivity profile from long-period magnetotelluric sounding using Hawaii-to-California submarine cable data, *J. Geophys. Res.*, *100*(B9), 17,837–17,854.
Mackwell, S. J., and D. L. Kohlstedt (1990), Diffusion of hydrogen in olivine: Implications for water in the mantle, *J. Geophys. Res.*, *95*(B4), 5079–5088.
McCluskey, M. D., M. C. Tarum, and S. T. Teklemichael (2012), Hydrogen in oxide semiconductors, *J. Mater. Res.*, *27*(17), 2190–2198.
Mosenfelder, J. L., N. I. Deligne, P. D. Asimow, and G. R. Rossman (2006a), Hydrogen incorporation in olivine from 2–12 GPa, *Am. Miner.*, *91*, 285–294.
Mosenfelder, J. L., T. G. Sharp, P. D. Asimow, and G. R. Rossman (2006b), Hydrogen incorporation in natural mantle olivines, in *Earth's Deep Water Cycle, Geophys. Monogr. Ser.*, vol. 168, edited by S. D. Jacobsen and S. Van Der Lee, pp. 45–56, AGU, Washington D. C.
Naif, S., K. Key, S. Constable, and R. L. Evans (2013), Melt-rich channel observed at the lithosphere-asthenosphere boundary, *Nature*, *495*, 356–359.
Neal, S. L., R. L. Mackie, J. C. Larsen, and A. Schultz (2000), Variations in the electrical conductivity of the upper mantle beneath North America and the Pacific Ocean, *J. Geophys. Res.*, *105*(B4), 8229–8242.
Otsuka, K., and S. Karato (2011), Control of the water fugacity at high pressures and temperatures: Applications to the incorporation mechanisms of water in olivine, *Phys. Earth Planet. Inter.*, *189*, 27–33.
Padrón-Navarta, J. A., J. Hermann, and H. O'Neill (2014), Site-specific hydrogen diffusion rates in Forsterite, *Earth Planet. Sci. Lett.*, *392*, 100–112.
Paterson, M. S. (1982), The determination of hydroxyl by infrared absorption in quartz, silicate glasses and similar materials, *Bull. Mineral.*, *105*, 20–29.
Peslier, A. H., A. B. Woodland, D. R. Bell, and M. Lazarov (2010), Olivine water contents in the continental lithosphere and the longevity of cratons, *Nature*, *467*, 78–81.
Philibert, J. (1991), *Atom Movements—Diffusion and Mass Transport in Solids*, Les Éditions de Physique, Les Ulis, Paris.
Poe, B. T., C. Romano, F. Nestola, and J. R. Smyth (2010), Electrical conductivity anisotropy of dry and hydrous olivine at 8 GPa, *Phys. Earth Planet. Inter.*, *181*, 103–111.
Schock, R. N., A. G. Duba, and T. J. Shankland (1989), Electrical conduction in olivine, *J. Geophys. Res.*, *94*(B5), 5829–5839.
Schultz, A., R. D. Kurtz, A. D. Chave, and A. G. Jones (1993), Conductivity discontinuities in the upper mantle beneath a stable craton, *Geophys. Res. Lett.*, *20*(24), 2941–2944.
Sifré, D., E. Gardés, M. Massuyeau, L. Hashim, S. Hier-Majumder, and F. Gaillard (2014), Electrical conductivity during incipient melting in the oceanic low-velocity zone, *Nature*, *509*, 81–85, doi:10.1038/nature13245.
Simpson, F., and A. Tommasi (2005), Hydrogen diffusivity and electrical anisotropy of a peridotite mantle, *Geophys. J. Intter.*, *160*, 1092–1102.
Stixrude, L., and C. Lithgow-Bertelloni (2005), Mineralogy and elasticity of the oceanic upper mantle: Origin of the low-velocity zone, *J. Geophys. Res.*, *110*, B03204, doi:10.1029/2004JB002965.
Stixrude, L., and C. Lithgow-Bertelloni (2007), Influence of phase transformations on lateral heterogeneity and dynamics in Earth's mantle, *Earth Planet. Sci. Lett.*, *263*, 45–55.
Tarits, P., S. Hautot, and F. Perrier (2004), Water in the mantle: Results from electrical conductivity beneath the French Alps, *Geophys. Res. Lett.*, *31*, L06612, doi:10.1029/2003GL019277.
Wanamaker, B. J., and A. G. Duba (1993), Electrical conductivity of San Carlos olivine along [100] under oxygen- and pyroxene-buffered conditions and implications for defect equilibria, *J. Geophys. Res.*, *98*(B1), 489–500.
Wang, D., M. Mookherjee, Y. Xu, and S. Karato (2006), The effect of water on the electrical conductivity of olivine, *Nature*, *443*, 977–980.
Withers, A. C., H. Bureau, C. Raepsaet, and M. M. Hirschmann (2012), Calibration of infrared spectroscopy by elastic recoil detection analysis of H in synthetic olivine, *Chem. Geol.*, *334*, 92–98.
Xu, Y., T. J. Shankland, and A. G. Duba (2000), Pressure effect on electrical conductivity of mantle olivine, *Phys. Earth Planet. Inter.*, *118*, 149–161.
Yang, X. (2012), Orientation-related electrical conductivity of hydrous olivine, clinopyroxene and plagioclase and implications for the structure of the lower continental crust and uppermost mantle, *Earth Planet. Sci. Lett.*, *317–318*, 241–250.
Yoshino, T., T. Matsuzaki, S. Yamashita, and T. Katsura (2006), Hydrous olivine unable to account for conductivity anomaly at the top of the asthenosphere, *Nature*, *443*, 973–976.

Yoshino, T., G. Manthilake, T. Matsuzaki, and T. Katsura (2008), Dry mantle transition zone inferred from the conductivity of wadsleyite and ringwoodite, *Nature*, *451*(17), 326–329, doi:10.1038/nature06427.

Yoshino, T., T. Matsuzaki, A. Shatskiy, and T. Katsura (2009), The effect of water on the electrical conductivity of olivine aggregates and its implications for the electrical structure of the upper mantle, *Earth Planet. Sci. Lett.*, *288*, 291–300.

Yoshino, T., M. Laumonier, E. McIsaac, and T. Katsura (2010), Electrical conductivity of basaltic and carbonatite melt-bearing peridotites at high pressures: Implications for melt distribution and melt fraction in the upper mantle, *Earth Planet. Sci. Lett.*, *295*, 593–602.

Yoshino, T., T. Matsuzaki, A. Shatskiy, and T. Katsura (2014), Corrigendum to "The effect of water on the electrical conductivity of olivine aggregates and its implications for the electrical structure of the upper mantle" [Earth Planet. Sci. Lett. 288 (2009) 291–300], *Earth Planet. Sci. Lett.*, *391*, 135–136, doi:10.1016/j.epsl.2014.02.016.